

Geometric Modeling of the Bench Dragon for Spiral Entry, Turnaround, and Exit Movements

Yutao Shen^{1*}, Xintong Shao² and Yilong Yang¹

¹School of Control Engineering, Northeastern University at Qinhuangdao, Qinhuangdao 066004, China

²School of Economics, Northeastern University at Qinhuangdao, Qinhuangdao 066004, China

***Corresponding author:**

Yutao Shen, School of Control Engineering, Northeastern University at Qinhuangdao, Qinhuangdao 066004, China.

Abstract

This paper focus on predicting the position and velocity of the "bench dragon" instances at every time during its equidistant spiral motion by geometric modeling. The "bench dragon" that a vital conventional folk activity in the Zhejiang-Fujian region is prevalent in the local. To enhance the contagious virtue and assist the dance acrobat team in adjusting their formations, the paper constructs a predictive model for the handlers' positions and velocities. In the first phase, based on available data, motion formulas are established to derive the curve of the front handler at the dragon's head, as well as the positional and velocity information for all handlers. The second phase, it involves overlap detection depending on polygon binarization and a greedy algorithm to identify collision positions and times, furthermore, determining the minimum spiral pitch under non-collision conditions. In the third phase, the complete motion path is assured of fixed spiral pitch and initial conditions. Additionally, polar coordinates are utilized to predict the positions and velocities of all handlers both before and after entering the turnaround space. Finally, the model is evaluated and summarized to assess its effectiveness and accuracy.

Keywords: Predictive Model, Overlap Detection, Polygon Binarization, Minimum Spiral Pitch, Turnaround Space.

Received: November 07, 2025;

Accepted: November 13, 2025;

Published: November 20, 2025

CCS: Applied Computing; Physical Sciences and Engineering; Mathematics and Statistics.

Introduction

The "bench dragon" that a traditional folk activity from the Zhejiang-Fujian region is composed of a hundred interconnected benches forming a spiraling dragon. The performance's appeal is relied on the compactness of the spiral and the movement speed. Typically, a "bench dragon" has 223 benches, including one head, 221 body sections, and one tail. The head bench is 341 cm long, while each body and tail section are 220 cm long and 30 cm wide. Furthermore, each bench features two small holes with 5.5 cm in diameter, positioned 27.5 cm from the head end. Virtually, benches are connected by specialized handles, creating the dynamic dragon [1-3].

During performances, the constituents of the team must move in a clockwise equidistant spiral with handle centers aligned along the spiral. To avoid collisions between the head and body, the team must switch from clockwise to counterclockwise motion in the turnaround space. Variations in initial position, spiral pitch, and head speed affect the team's trajectory [4-6]. Therefore, analyzing the handles' motion is crucial to enhance performance and ensure smooth execution.

To address the concern, we propose a model for predicting handle positions and velocities. The main contributions of this paper are:

- Construct a two-dimensional geometric model to predict the positions and velocities of the front handle centers which are following an equidistant spiral trajectory at every time.
- Application of a greedy algorithm and polygon binarization to perceive

Citation: Yutao Shen, Xintong Shao, and Yilong Yang (2025) Geometric Modeling of the Bench Dragon for Spiral Entry, Turnaround, and Exit Movements. J Modr Sci Scient Res 1: 1-6.

collisions and calculate the minimum spiral pitch for the fixed turnaround region [7-9].

- Analysis of the turnaround space's curve and simulation of the positions, as well as velocities of the front handle of the dragon body and the rear handle of the tail throughout the motion process.

System Model

The model constructed in this article consists of three stages:

- In the first stage, we explored the motion patterns of the dragon head, body segments, and tail along equidistant helical curves with a constant pitch. On the premise of ensuring that the starting position of the front handle of the faucet is fixed and the spiral pitch remains unchanged, their motion trajectory and position coordinates were calculated using geometric functions. Next, based on the length information of the workbench and various constraint conditions, the position coordinates of other handles were determined. Finally, based on these coordinate data, the velocity values for each time node were calculated.
- The goal of this stage is to determine the moment of collision and ensure that the dragon dance team can smoothly maneuver within the limited space. We first start from the circumference of the outermost spiral trajectory to reduce the potential collision area, and then use greedy algorithms and polygon binarization techniques to simplify the collision problem into an overlap detection task. Based on this, we simulated the collision between various parts of the body and the dragon head in the dragon dance team, as well as the specific time of the collision. At the same time, we also set a circular turning area and calculated the minimum spiral spacing distance required for the faucet to enter the turning area.
- In the third stage, we focused on the S-shaped turning path and conducted in-depth analysis of the position and speed data of the dragon dance team before and after the turning space. On the premise of maintaining a constant spiral spacing and assuming symmetry between the inlet and outlet spirals, we have clarified the turning behavior of the faucet in a specific space. Through geometric principles, we calculated the actual values of the angle and radius of the arc, and constructed a polar coordinate system. Finally, we obtained the mathematical relationship between radial distance and angle over time. Based on this, we obtained the dynamic polar coordinate trajectory of the front handle of the faucet over time, and further calculated the position and velocity information of all handles.

First Stage

We set the initial radius $r_{in} = r_A = 16 \times 0.55 \text{ m} = 8.8 \text{ m}$, the constant velocity of the dragon head's front handle $v = 1 \text{ m/s}$, and the spiral pitch $r_0 = 0.55 \text{ m}$. We analyze the position and velocity of the front handles of the dragon's head, body sections, and tail from the start until 300 seconds. At time t , if the front handle of the dragon head reaches Position B (where B is any allowable position), the velocity v is decomposed into two components: v_1 towards the spiral's center O, and v_2 perpendicular to v_1 . The angle θ between v_1 and the x-axis is θ (with a clockwise direction as positive). The distance from Point B to O is r , with the initial distance $r_{in} = r_A$ and the spiral pitch r_0 . The situation is depicted in Figure 2.

Details are illustrated in Figure 1.

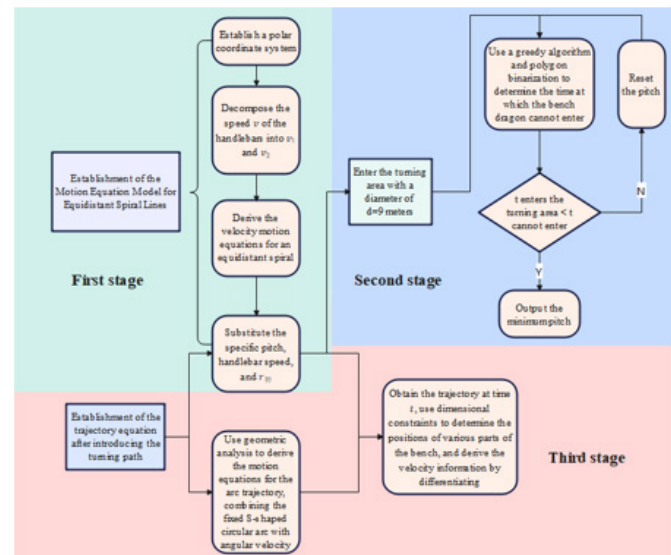


Figure 1: System model mind map

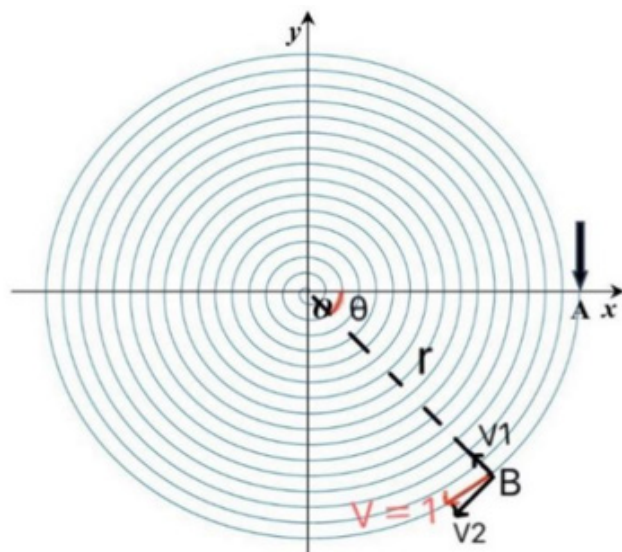


Figure 2: Velocity decomposition of the dragon head's front handle at time t .

The following equations can be established

$$\begin{cases} r = r_{in} - \frac{r_0 \theta}{2\pi} \\ \frac{dr}{dt} = v_1 \\ \frac{d\theta}{dt} = \frac{v_2}{r} \\ v_1^2 + v_2^2 = v^2 \end{cases} \quad (1)$$

Given $r_{in} = r_A = 16 \times 0.55 \text{ m} = 8.8 \text{ m}$, simplifying Eq. (1) yields:

$$v = -\sqrt{1 + \frac{4\pi^2}{r_0^2} r^2} \frac{dr}{dt} \quad (2)$$

Substituting $v = 1 \text{ m/s}$ into Eq. (2), we obtain:

$$\begin{cases} t = -\frac{r}{2} \sqrt{1 + \frac{4\pi^2}{r_0^2} r^2} - \frac{r_0}{4\pi} \operatorname{asinh}\left(\frac{2\pi r}{r_0}\right) + C \\ \theta = 32\pi - \frac{2\pi}{r_0} r \end{cases} \quad (3)$$

where the spiral pitch $r_0 = 0.55$ m, C is a constant of approximately 442.59 (calculated with $t = 0$ s, $r_0 = 0.55$ m, and $r = 8.8$ m), and asinh is the inverse hyperbolic sine function. For a given t , Eq. (3) determines the value of r at each moment, providing the trajectory of the front handle of the dragon's head and the first body section. The results are shown in Figure 3.

Substituting r into Eq. (3) yields the angle θ . Using the following equation, the coordinates of the front handle of the dragon's head at time t can be determined.

$$\begin{cases} x = \cos\theta * r(t) \\ y = -\sin\theta * r(t) \end{cases} \quad (4)$$

The coordinates of the remaining handles can be derived based on the following conditions:

- The distance between the rear and front handles remains constant, where the front handle of the subsequent bench coincides with the rear handle of the preceding bench.
- All handles are aligned along the spiral trajectory.
- The front handle of a following bench is oriented clockwise and positioned behind the front handle of the previous bench.

Given the coordinates at time t , the velocities of each handle at t seconds can be calculated using Eq. (5):

$$\sqrt{\left(\frac{dy}{dt}\right)^2 + \left(\frac{dx}{dt}\right)^2} = v \quad (5)$$

This yields the positions and velocities of the centers of all handles in the dragon dance team.

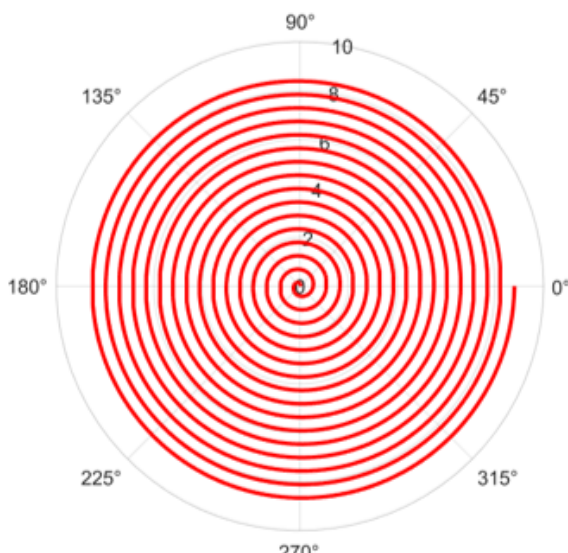


Figure 3: Trajectory of the Front Handle of the Faucet in Polar Coordinates

Second Stage

Collision Problem

The study focuses on the scenario where the head of the dragon can no longer coil inward. The optimization problem of determining when the dragon's head collides with the body can be simplified to finding when the head overlaps with a particular segment of the body. This problem can be solved using a greedy algorithm combined with polygon binarization. The results are shown in Figure 4.

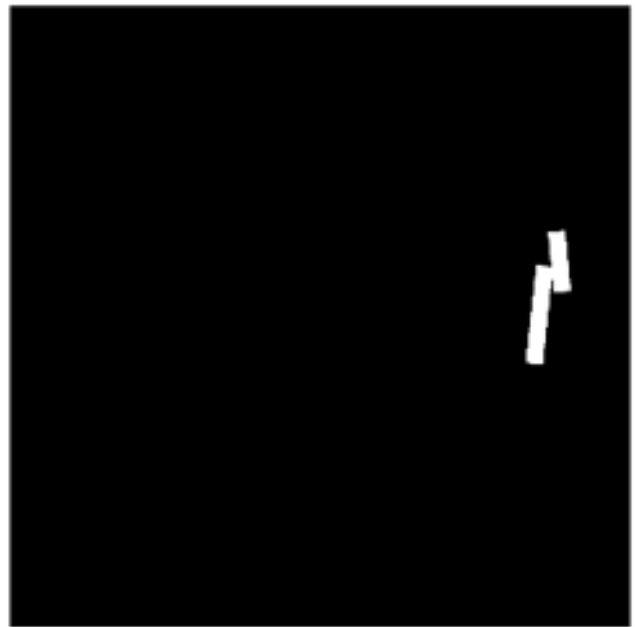


Figure 4: Schematic Diagram of the Pixel Collision between the Dragon's Head and the 31st Segment of the Dragon's Body

Taking the moment when the dragon's head coils inward as $t = 0$, and testing with a step size of 0.0000001, the collision is found to occur at $t = 54.0381020$. Substituting t into Eq. (3) from the first phase, the value of r is obtained. By following the steps of the basic model, the position and velocity information can be calculated accordingly.

Minimum Pitch Problem

Based on the study of the minimum pitch required for entry into a fixed circular turning area, with the center of the spiral as the origin, this research investigates the conditions for entering the turning space. According to Eq. (2), in order to simplify the model and easily determine the motion trajectories of both the dragon's head and body segments, the velocity v is assumed to be 1 m/s. The required turning space is defined as a circular area with a diameter of 9 meters, centered at the spiral's origin. If the dragon's head enters the space tangentially, it must satisfy two conditions simultaneously:

$$V_1 = 0, \text{ which means } \frac{dr}{dt} = 0$$

$$r = 4.5 \text{ m}$$

According to Eq. (3), differentiating r with respect to t yields:

$$\frac{dt}{dr} = -\frac{1}{2v} \sqrt{1 + \frac{4\pi^2}{r_0^2} r^2} - \frac{2\pi^2 r^2}{v r_0^2 \sqrt{1 + \frac{4\pi^2}{r_0^2} r^2}} - \frac{1}{2v \sqrt{1 + \frac{4\pi^2}{r_0^2} r^2}} \quad (6)$$

After substituting $r = 4.5$ m into Eq. (6), the result becomes a constant with respect to r_0 , which does not satisfy the condition of tending to infinity. Therefore, Condition One is not met, and the dragon's head cannot coil into the turning space tangentially; it must enter the turning space by intersecting the boundary.

The study then focuses on the intersection point between the equidistant spiral path of the dragon's head and the boundary of the turning space. In Eq. (3), t is a function of r , r_{in} , and r_0 . For the dragon's head to successfully enter the turning space, the time at which it enters must be earlier than the collision time. This can be expressed as:

$$-\frac{9}{4} \sqrt{1 + \frac{81\pi^2}{r_0^2}} - \frac{r_0}{4\pi} \operatorname{asinh}\left(\frac{10\pi}{r_0}\right) + \frac{r_{in}}{2} \sqrt{1 + \frac{4\pi^2}{r_0^2} r_{in}^2} + \frac{r_0}{4\pi} \operatorname{asinh}\left(\frac{2\pi r_{in}}{r_0}\right) < 382.8 \quad (7)$$

By setting r_{in} within the range $(32/\pi, 64/\pi)$ and substituting the initial value of r_{in} into the equation, it is determined that the dragon's head will collide with the 22nd segment of the body, with the minimum pitch being 0.65 m. The results indicate that, in practical tests, the size of r_{in} does not affect the final value of the minimum pitch.

Third Stage

Minimum Pitch Problem

The turning path is characterized by an S-shaped curve, which is constructed from two arcs that are tangentially connected. Notably, the radius of the initial arc is double that of the subsequent arc. This path maintains tangency with both the inward and outward spirals. As the dragon's head approaches the turning space, it intersects the boundary and shifts from an equidistant spiral trajectory to a uniform circular motion. Within the turning space, the direction of movement is altered along the S-shaped curve, transitioning from a clockwise to a counterclockwise orientation. Upon reaching the circular boundary once more, the dragon's head reverts from uniform circular motion back to equidistant spiral motion, ultimately exiting the turning space.

Due to the dragon's head's inability to enter the turning space tangentially, the S-shaped curve cannot be formed by two semicircles. Instead, it is composed of two minor arcs.

Let the entry and exit points be denoted as M and N, respectively. The centers of the first and second arcs are identified as O_1 and O_2 , with the arcs intersecting at Point P. Perpendicular lines are drawn from O_1 and O_2 to the diameter of the circular region, intersecting at Points C_1 and C_2 . The radii of the larger and smaller arcs are defined as r_1 and r_2 , respectively, with the relationship $r_1 = 2r_2$. The angle formed between the tangent of the inward spiral at Point M and the tangent direction of the circular region at the same point is labeled as α . Additionally, the angles between O_1C_1 and O_1O_2 , and between O_1M and MN , are designated as β and γ , respectively, as depicted in Figure 5.

Model Assumptions

Taking the start of the turn as the reference time $t = 0$, and assuming that the dragon's head handle begins coiling inward 100 seconds earlier, it can be calculated that the initial distance of the head handle from the center of the spiral is greater than 10.35 meters, i.e., $r_{in} > 10.35$ m. In this study, the selected r_{in} falls within the range of (12, 15) meters.

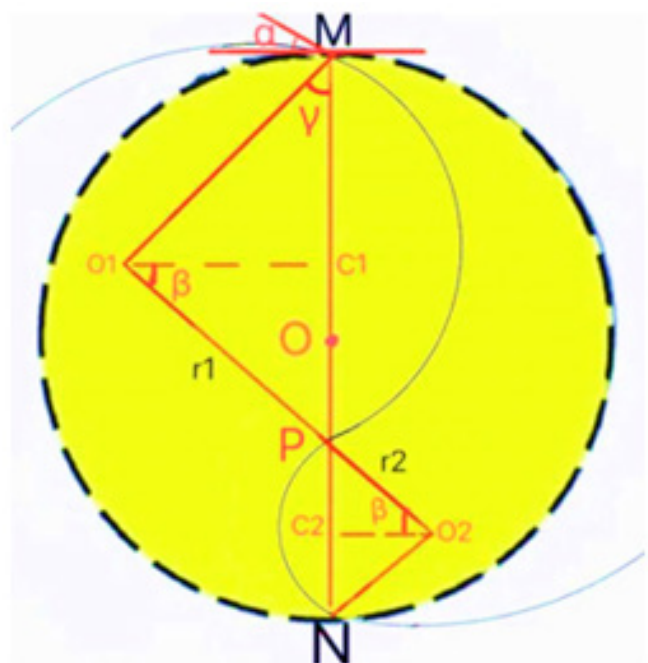


Figure 5: Schematic Diagram of the Turning Path

Model Construction

To facilitate solving the problem using geometric relationships, a Cartesian coordinate system is established with the origin at Point O, appropriately positioned as shown in Figure 6.

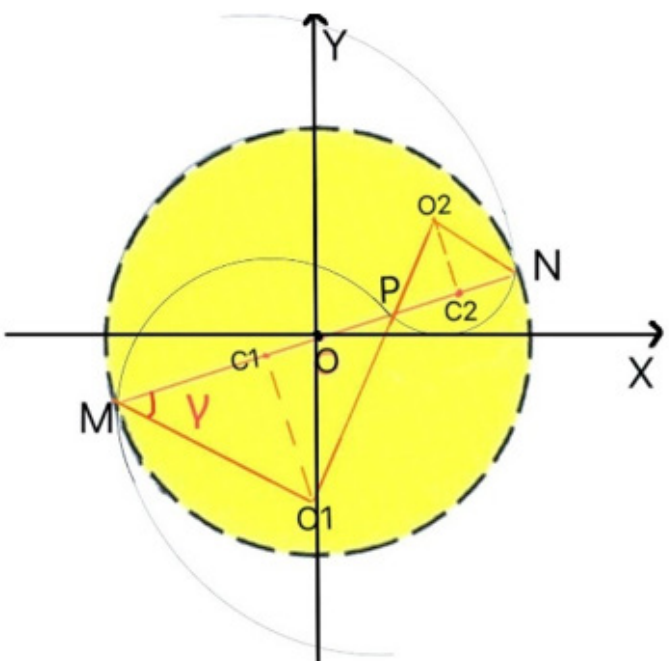


Figure 6: Turning Path in the Rectangular Coordinate System

Based on geometric relationships, the angle γ is calculated to remain constant at 0.554325 radians. Similarly, the radii of the two arcs are fixed, with $r_1 = 3.005384$ m and $r_2 = 1.502692$ m. When r_{in} is varied, the entry point of the dragon head's trajectory within the turning region shifts in the xy-coordinate system. Nevertheless, this variation does not influence the constant value of γ or the radii of the arcs. The arcs cannot be modified without disrupting their tangency at all points, implying that the turning curve cannot be compressed. Consequently, there

exists only one feasible path for the turning curve, as depicted in Figure 7.

Upon completing the first half of the arc, a new polar coordinate system is introduced. The dragon's head handle enters the first half of the arc at Point M and progresses to Point $H_1(r; \theta)$, with the arc's center located at $O_1(r_0, \theta_0)$. In this context, r_0 no longer corresponds to the spiral's pitch. The angles θ , θ' , θ_b , and θ_{bin} are defined as illustrated in Figure 8.

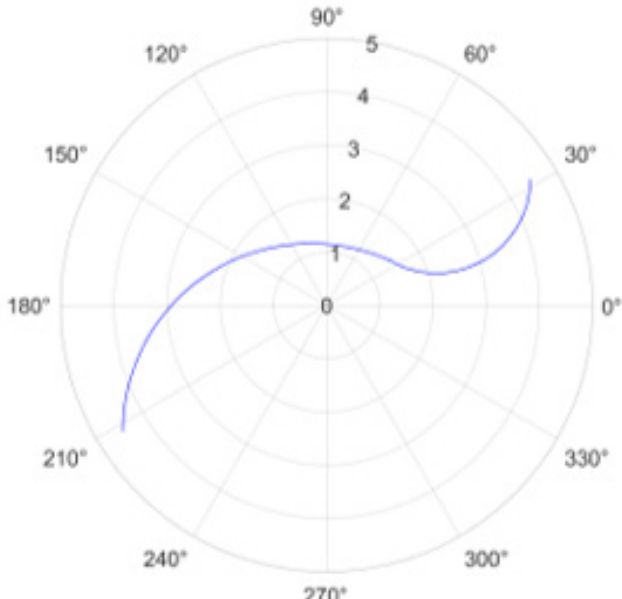


Figure 7: Dynamic Polar Coordinate Trajectory of the Dragon's Head Handle in the Turning Region

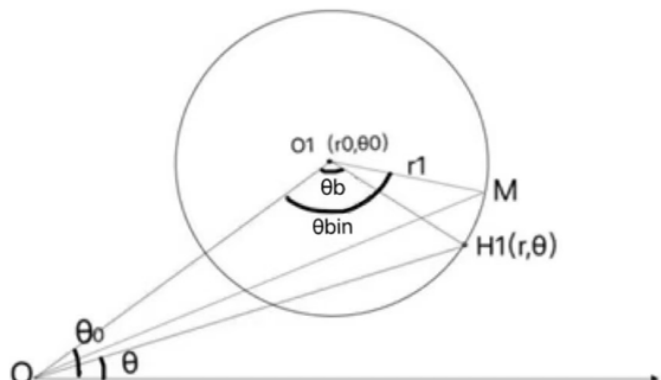


Figure 8: Schematic Diagram of the Polar Coordinate Position Relationship of the Dragon's Head Handle During Motion on the First Half of the arc

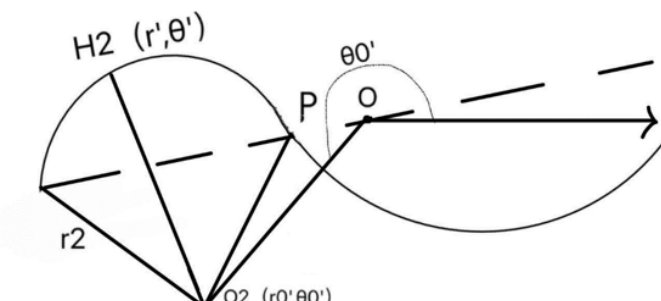


Figure 9: Schematic Diagram of the Polar Coordinate Position Relationship of the Dragon's Head Handle During Motion on the Second Half of the arc.

Based on the geometric relationships, the expression for θ as a function of t can be derived. By adopting the methodology employed for solving the first half of the arc, a polar coordinate system is established, as depicted in Figure 9.

In triangle OPO_2 , the cosine law is utilized to derive the expression for θ' as a function of t . By employing the methodology applied in the initial phase, the position and velocity outcomes are determined.

Using an initial radius $r_{in} = 12$ m and a constant handlebar speed of $v = 1$ m/s, the resulting graph for the time interval from -50 s to 100 s is generated by applying the equations for the circular arc and equidistant spiral, as illustrated in Figure 10.

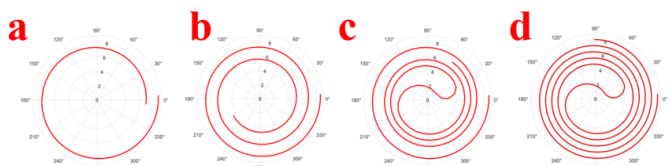


Figure 10: The Trajectory of the Front Handlebar Turn-in at (a) -50 s Lead Moment, (b) 0 s Lead Moment, (c) 50 s Lead Moment, and (d) 100 s Lead Moment

Model Evaluation

Advantages

The following advantages are possessed by the motion geometry simulation model constructed in this article:

- Compared to Cartesian coordinate system, using polar coordinates greatly simplifies the calculation process and accelerates the model construction process.
- The equation model constructed based on geometric characteristics is theoretically considered correct and reliable.
- With the help of the trajectory diagram of the dragon head handle at different time points t , this model cleverly solves the complex classification problem of which parts of the dragon body still maintain spiral motion at specific times and which parts have transformed into circular motion.

Disadvantages

When drawing the trajectory diagram of the faucet handle over time t , it was determined with a time accuracy of 0.0001 seconds based on the positional relationship between the faucet and the body size. However, unfortunately, the program has low efficiency and insufficient accuracy. Neural networks could be employed to obtain the trajectory diagrams of the dragon's head handle [10,11]. After determining the positional relationship between the dragon head and the body based on their size, the speed can be further calculated through differential operations.

The parameters set in this article, such as starting radius, spiral spacing, and speed, are all based on specific situations, and may need to be adjusted according to different performance venue conditions, team size, and specific performance needs in practical applications. In future work, we will train and optimize collision detection algorithms based on actual performance data, aiming to improve their detection accuracy and stability.

Conclusion

This paper presents a motion model of the bench dragon, which coils inward and outward along an equidistant spiral, to analyze the position and velocity of each dragon segment, as well as the head and tail handles, at various time points. The model incorporates an ideal circular turning area and employs a greedy algorithm combined with polygon binarization to detect rectangle overlap, enabling the identification of collision conditions for the bench dragon as it enters the turning area. Additionally, the spiral pitch conditions required for entering the turning area are elucidated.

The study reveals that varying initial distances r_{in} (the distance from the spiral center to the starting position of the dragon's head handle) do not influence the turning path. This path is characterized by an S-shaped curve composed of two tangentially connected arcs, with the radius of the first arc being twice that of the second. These arcs maintain tangency with both the inward and outward spirals. By specifying the velocity of the dragon's head handle, the position and velocity of each dragon segment, along with the head and tail handles, are determined at different times along the equidistant spiral and the arcs' trajectories.

The proposed model assumes a constant speed for the dragon's head and body during spiral motion, with the dragon's segments being rigidly connected. However, in real-world performances, factors such as human-driven forces and environmental conditions may introduce variations in speed and shape. Future work will focus on incorporating these dynamic changes in speed and shape, as well as developing more sophisticated motion equations to accurately describe these variations.

References

1. Pan D, Sirisuk M (2023) Collective memory construction and educational inheritance of ritual practices of bench dragon performance in Pujiang, China: Educational inheritance of ritual practices of bench dragon performance. *International Journal of Curriculum and Instruction* 15: 2232-2250.
2. Zhang W, Wan W, Wang W (2024) The evolution and review of the cultural ecology of village sports performances: A study on the "Bench Dragon" in Chongren. *Academic Journal of Humanities & Social Sciences* 7: 18-23.
3. Mingna S H I, Liangliang S U N (2015) Traditional village sports culture from the perspective of cultural ecology research--Taking provincial intangible cultural heritage Anren bench dragon in Sichuan as an example. *Journal of Chongqing Jiaotong University Social Sciences Edition* 15: 105.
4. Nho J, Jang T, Sohn S H (2024) Spiral trajectory of satellites subjected to drag forces in the atmosphere. *The Physics Teacher* 62: 510-514.
5. Kang H, Zang Y, Wang X, Chen Y (2022) Uncertainty-driven spiral trajectory for robotic peg-in-hole assembly. *IEEE Robotics and Automation Letters* 7: 6661-6668.
6. Huang R, Huang X, Wang D, Yang L (2022) Effect of Swing-Spiral-Trajectory on pulsed fiber laser welding stainless steel/Copper dissimilar metals. *Optics & Laser Technology* 156: 108516.
7. Gupta V (2024) Greedy algorithm for multiway matching with bounded regret. *Operations Research* 72: 1139-1155.
8. Gokalp O (2020) An iterated greedy algorithm for the obnoxious p-median problem. *Engineering Applications of Artificial Intelligence*, 92: 103674.
9. Wang C, Pan Q K, Jing X L (2024) An effective adaptive iterated greedy algorithm for a cascaded flow shop joint scheduling problem. *Expert Systems with Applications* 238: 121856.
10. Suo Y, Chen W, Claramunt C, Yang S (2020) A ship trajectory prediction framework based on a recurrent neural network. *Sensors* 20: 5133.
11. Zhang X, Mahadevan S (2020) Bayesian neural networks for flight trajectory prediction and safety assessment. *Decision Support Systems* 131: 113246.

Copyright: © 2025 Yutao Shen. This is an open-access article distributed under the terms of the Creative Commons Attribution License, which permits unrestricted use, distribution, and reproduction in any medium, provided the original author and source are credited.